Nanoscale

Accepted Manuscript

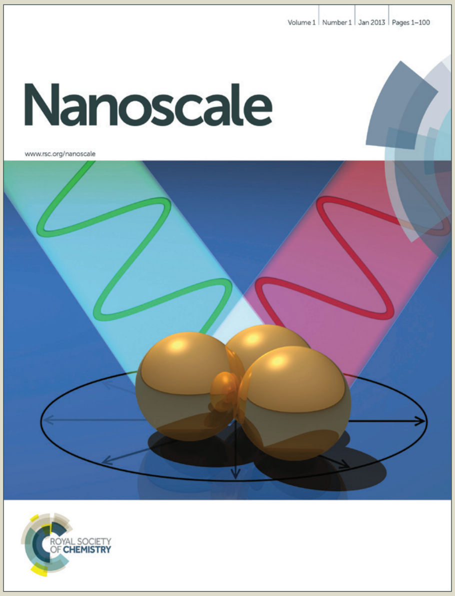

ROYAL SOCIETY OF CHEMISTRY

www.rsc.org/nanoscale

Annealing-free, long-term reliable and strongly adhesive silver nanowire networks by introduction of nonconductive and biocompatible polymer binder

*Yunxia Jin, Dunying Deng, Yuanrong Cheng, Lingqiang Kong, Fei Xiao**

Department of Materials Science, Fudan University, 220 Handan Road, Shanghai 200433, China

*Phone: +86-21-65642110. *E-mail: feixiao@fudan.edu.cn

ABSTRACT

As a promising candidate to replace the brittle and expensive transparent indium tin oxide (ITO) conductor, silver nanowire (AgNW) networks still involving issues of high-temperature post-treatment and poor substrate adhesion for industrial application. Here a room-temperature soldering, one-step solution method is developed to achieve high-performance Ag nanowire transparent conductive film (TCF). A nonconductive binder is prepared from poly(dopamine) and alginic acid which contain abundant catechol and carboxylic acid functional groups. The drying of the binder on Ag nanowire percolation networks induces tighter contact among nanowires and strong adhesion to the substrate, simultaneously enhancing the electrical and mechanical properties without high-temperature annealing process. As a result, highly conductive and bendable AgNW film is demonstrated on low-cost polyethylene glycol terephthalate (PET) substrate, showing an 89% optical transmittance at $\lambda = 550$ nm with a 16.3 Ohm sq^{-1} sheet resistance. Its optical and electrical performance is superior to that obtained from the reported indium tin oxide (ITO) films. Moreover, the AgNW film exhibits strong adhesion to the substrate, maintaining its conductivity after 100 times of tape tests, and still resisting tape test even exposure to solvent for several hours. Most importantly, the film shows good reliability during long-term 85 °C/85%RH aging, which has been rarely investigated although it is a critical requirement for industrial application. The encouraged comprehensive features of the prepared AgNW film greatly contribute to its use as transparent electrodes in multifunctional flexible electronic devices.

Introduction

As the rapid development of flexible smart electronics, an industrial demand for low-cost, flexible and highly transparent conductive film (TCF) to replace the expensive and brittle ITO-sputtered electrodes has been stimulated. Candidates include conducting polymer,[1-3] carbon nanotubes (CNTs),[4, 5] graphene,[6, 7] metal grids[8, 9] and metallic nanowires.[10-12] As the performance of these TCFs, optical transmittance (T) and electrical sheet resistance (R_s) are extremely important, and the specification varies based on application. For example, 10^6 Ohm sq^{-1} is sufficient for antistatic applications, 400−1000 Ohm sq^{-1} is enough for many touch screen applications, and $\leq$ 15 Ohm sq^{-1} is needed for solar cells.[13, 14]

TCFs based on carbon materials or conducting polymer usually have a relatively high sheet resistance at high transmittance, and fail to fulfill the requirement of high performance optoelectronic devices.[15] Silver nanowires (AgNWs), however, show comparable electrical conductivity with that of metallic oxides, and become the most promising ITO substitute. Such use of AgNWs has been reported by many researchers, including the possibilities for application as transparent electrodes in optoelectronic devices. [10, 16, 17]

But for large-scale fabrication of AgNWs film several issues should be addressed. First, the resistance of wire-wire junction is too large due to the insulating coating of poly(vinyl pyrrolidone) (PVP) on the surface of Ag nanowire and the loose contact among AgNWs. Subsequently, a high-temperature thermal annealing or mechanical pressing is often required, and hence limits the choice of substrates and device fabrication in terms of thermal and mechanical endurance.[4, 18, 19] Second, AgNWs are easily detached from the deposited bare substrate due to the weak adhesion. Several strategies have been proposed for these issues, such as conformal pressure applying,[10] surface encapsulation,[10, 11, 20] and high-intensity pulsed light sintering.[21] However, these methods are high energy consumption or time-consuming for rapid production process. Moreover, most reported methods only address one of the above issues and their applications are restricted to certain kinds of devices.

To obtain synchronous adhesion and electrical conductivity, Lee et al. introduced conducting polymer poly(3,4-ethylenedioxythiophene):poly(styrenesulfonate) (PEDOT:PSS) to the top layer of AgNW film as nano-soldering materials by a two-step process. The resultant

AgNW composite film exhibited a sheet resistance of 25~54 ohm sq^{-1} for T = 90% at 550 nm with an enhanced adhesion.[22] This suggests a possible method for reinforced performance of AgNW film by introducing polymer as binder. But from a practical point of view, this polymer should be critically selected. Because the polymer adhesive located on the AgNW surface usually improved the adhesion of AgNW to substrate, but accompanying with the sharp reduction of the conductivity. Furthermore, on the one side, the polymer adhesive is expected to be soluble or well-dispersed in low-volatile and polar solvent of AgNW dispersion, such as alcohol, isopropyl alcohol or water, so as to maintain the solution-process of AgNW film deposition. But on the other side, this polymer adhesive is expected to be resistant to various solvents to perform good adhesion during the following solution processes of device fabrication and high humidity to achieve long-term reliability. The above requirements of the polymer adhesive seem to contradict with each other.

In this paper, we developed a novel hybrid AgNW dispersion using nonconductive mussel-inspired biocompatible complex as binder to obtain high-performance transparent electrode via simple and rapid one-step spray coating without annealing. Since elegantly demonstrated by Messersmith and co-workers,[23] poly(dopamine) (PDA) have attracted much attention for excellent chemical stability and good adhesion to virtually all types of surfaces, and even to wet surface. Akter et al. introduced poly(dopamine) onto substrate of polydimethylsiloxane (PDMS), demonstrating a good adhesion of spray-coated AgNW film to the modified substrate with a sheet resistance of 35 Ohm sq^{-1} at transmittance of 80%.[24] Besides, taking note of studies that indicated the possible effectiveness of carboxylic acid group in contributing the electrical conductivity of metal particles during sintering,[25, 26] here we prepared a complex of poly(dopamine) with alginic acid (Aa) intending to achieve synchronous adhesive and conductive AgNW composite film. Because Aa is the only polysaccharide containing carboxyl groups in each constituent residue.[27] It is known that both pure PDA and Aa are not soluble in any inorganic or organic solvent, which is significantly preferred for fabricating stable AgNW composite. However, Aa-PDA obtained good solubility in AgNW dispersion with a little bit of addition of ammonia, which enabled the solution processing of AgNW film fabrication. Meanwhile, the little amount of ammonia can be easily removed due to its high volatility, consequently release the favorable poor solubility of Aa-PDA after AgNW film deposition. As a result, the prepared AgNW composite film exhibited a 16.3 Ohm sq^{-1} sheet resistance at $T \sim 89\%$ with a good adhesion and solvent resistance, outperforming other transparent conducting materials. And most importantly, the performance nearly showed no change during the long-term 85 °C/85%RH aging. We note that this is the first positive report about the reliability of AgNW composite film. Besides, both Aa and PDA are biocompatible, enabling the potential application in bioelectronics.

Experimental

AgNW dispersed in ethanol with a concentration of 10 mg mL^{-1} were purchased from Blue Nano. The mean length and diameter were 15 μm and 40 nm, respectively. Dopamine hydrochloride (Aladdin Reagent Co.) was added into ammonia (25-28 wt%) till 2.5 mg mL^{-1}. Subsequently, alginic acid (Aladdin Reagent Co.) was also added (14.5 mg mL^{-1}) into the solution. The monomer dopamine spontaneous polymerized to poly(dopamine) in ammonia, and formed complex with aginic acid. The mixture was allowed to react for 12 h, and a uniform dark solution was obtained. Ethanol was added into the solution for the precipitation of the complex and the mixture was centrifuged at 8000 rpm for 3 min. The as-obtained complex was washed by ethanol with a little water once more. At last, Aa-PDA was added into the AgNW dispersion, and the solution was diluted with mixed solvent of water and ethanol at a weight ratio near 1:1. In the final solution, AgNW was 0.65 mg mL^{-1} and Aa-PDA was 0.07 mg mL^{-1}.

The resultant dispersion was sprayed onto polyethylene terephthalate (PET) using a U-star airbrush. The spray conditions, such as nozzle-to-substrate distance, spraying nozzle diameter, spraying pressure were the key parameters for the spray coating process. Too small nozzle diameter and spraying pressure will cause the relative long Ag nanowires to form circles and more stack boundaries due to the small droplet form nozzle, which reduced the electrical conductivity of AgNW film. In this study, the spray conditions were maintained at 25-30 cm distance between nozzle and substrate, 0.3 mm nozzle diameter and 0.6 MPa spraying pressure. Since the dispersion was volatile, we did not need to heat the substrate to accelerate the evaporation of the fine droplets on the substrate. When the distance between nozzle and substrate was decreased, the substrate can be heated at 50 °C on a hotplate in an effort to promote the evaporation of solvent.

Infrared spectra were obtained by Fourier transform infrared (FTIR, NEXUS-470). The micrographs were obtained using a field emission scanning electron microscope (FE-SEM, JEOL, JSM-6701F). Optical transmission spectra were obtained by a T6 new century spectrophotometer (PGeneral, China) with bare PET substrate as a reference. X-ray photoelectron spectroscopy (XPS) analysis was carried out on a Kratos axis ultra DLD electron spectrometer. Al Kα radiation was used as the X-ray source and operated at 160 eV for full spectrum and 40 eV for element spectrum. The weight loss versus temperature was measured by thermogravimetric analyzer (TGA7, PE) with a heating rate of 10 °C min^{-1}. The sheet resistance was measured using a four-point probe system (SB100A/20A, Shanghai Qianfeng), and obtained from the averaged values of several positions on a sample. The adhesion strength of AgNWs film was investigated by a 90° peeling test. A 12-mm-wide 3M scotch tape was attached to an electrode sample, and then peeled off from the sample. The process was repeated for 100 times using a new tape for every test, and the adhesion property of the AgNW films was evaluated by measurement of sheet resistance after tape test. The long-term reliability tests of AgNWs films followed the test standard in microelectronics, in which the test temperature and humidity is defined as 85 ^{o}C and 85% RH.

Results and discussion

The structure of complex Aa-PDA was revealed by X-ray photoelectron spectroscopy (XPS) and Fourier transform infrared (FTIR). As shown in Fig. 1a, N 1s peak around 400 eV confirmed the coexistence of alginic acid and PDA. By contrast, no obvious N 1s peak was detected in pure Aa (Fig. 1b). The FTIR spectroscopies further demonstrate the interaction inside Aa-PDA. Alginic acid exhibits a broad absorption band around ~3400 cm^{-1} relating to O–H stretching vibration, a peak at ~1730 cm^{-1} corresponding to C=O stretching vibration, and a peak at ~1028 cm^{-1} relating to C-O-C asymmetric vibration. PDA shows a characteristic peak around 1600 cm^{-1} corresponding to the stretching of C=C and N–H deformation vibration, and similar peaks with alginic acid at ~3400 cm^{-1}. After complex formation, peak at ~1730 cm^{-1} corresponding to C=O can still be observed, indicating the residue of free –COOH groups. But the peaks at ~1600 cm^{-1} corresponding to COO^- (carboxylate) asymmetric vibrations, and ~1400 cm^{-1} corresponding to COO^- symmetric vibrations were observed. These provide firm evidence of a strong interaction between alginic acid and PDA, enabling the sharply improvement of solubility of Aa-PDA.

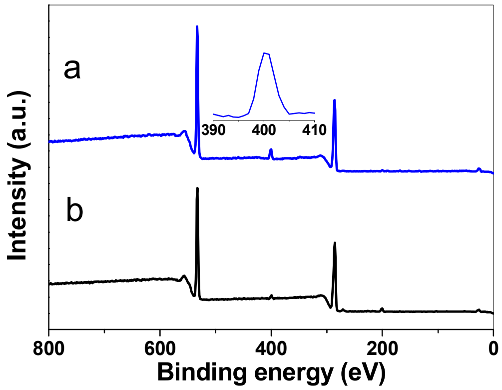

Fig. 1. XPS curves of (a) Aa-PDA (inset is the high resolution of N 1s peak) and (b)Aa.

The pure PDA only dissolves in strong alkali solvent whose pH value near 13, while the Aa-PDA exhibited good solubility in weak basic solvent with pH value close to 8. Thus, Aa-PDA can be directly used as an additive in AgNW dispersion due to the great promotion of solubility, enabling the solution-processed deposition technology of AgNW film. Moreover, it further confirmed the strong interaction between Aa and PDA. Besides, since there was no additional ammonia was added into Aa-PDA solution, the weak basic is supposed to be attributed to the ammonia residue during Aa-PDA preparation. At last, a uniform dispersion of Aa-PDA was obtained. During the following spray coating, the solubility of Aa-PDA became worse with the evaporation of ammonia, leading to possible good solvent and humidity resistance of AgNW/Aa-PDA film.

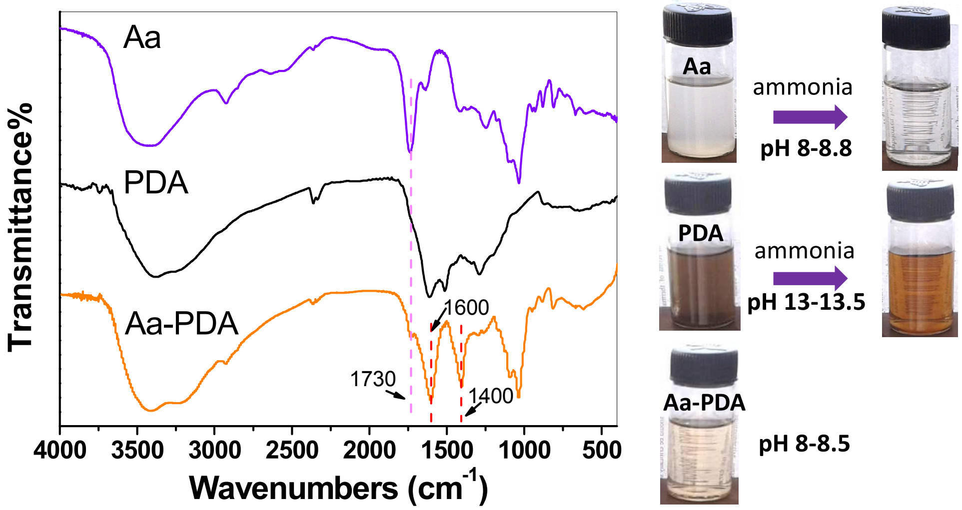

Fig. 2. FTIR spectra and the corresponding solubility in mixing solvent of water and alcohol of Aa, PDA and Aa-PDA. The visibility of letters behind bottles helped indicating the solubility. The pH values of the solution in right bottle determined by a pen pH meter. Aa solution became clear with only a bit of ammonia adding; PDA only dissolved in strong alkali solvent with pH value near 13-14; Aa-PDA maintained good solubility even in extremely alkalescent solvent.

Fig. 3a shows the photographs of pristine AgNW dispersion and its mixture with prepared Aa-PDA. There is no obvious change in appearance and viscosity. So it is convenient to follow the deposition technology of pure AgNW dispersion after Aa-PDA addition, removing the special care in case of severe property change caused by additives. Fig. 3b illustrates the schematic procedure of AgNW/Aa-PDA deposition. The mixture of AgNW and Aa-PDA was sprayed on a clean bare PET substrate at room temperature. After this extremely simple and fast process, a colorless and transparent film was obtained (Fig. 3c). By optimizing AgNW/Aa-PDA dispersion composition and deposition technology, we produced AgNW film with R_s around 16.3 Ohm sq^{-1} for T ~ 89% at λ = 550 (Fig. 3d). Its optoelectronic performance surpasses that of commercial ITO on PET.

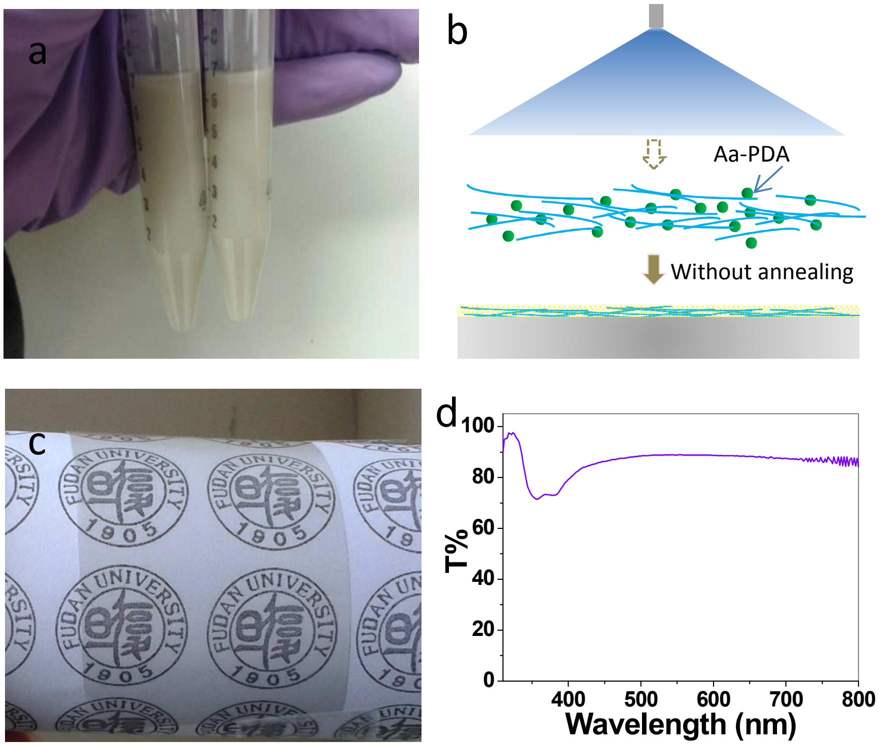

Fig. 3. Photographs of (a) AgNW dispersion (left) and its mixture with Aa-PDA

(right). (b) Schematic fabrication of transparent, conductive AgNW film by spray coating. (c) Photograph of AgNW film deposited on a PET substrate. (d) Optical transmittance of AgNW/Aa-PDA composite film with R_s = 16.3 Ohm sq^{-1}.

As shown in Fig. 4, the adhesion of AgNW composite film to PET substrate was studied. The sheet resistance of AgNW film sharply increased to ten times the original value just after two cycles of tape tests (curve a), while it only increased from 34.2 Ohm sq^{-1} to 42.4 Ohm sq^{-1} for AgNW/Aa-PDA composite film (curve b). It is noted that AgNW/Aa-PDA film still maintained its electrical conductivity after 100 times of tape tests, whose sheet resistance was only around three times the original value. The corresponding transmittance at 550 nm of AgNW/Aa-PDA was also measured after tape test. It shows a relatively fast increase from 92.5% to 93.3% after the first tape test, indicating a little silver nanowires were removed out. But the transmittance maintained constant in the range of 93.3% ~ 93.8% over the following 99 cycles of tape tests although the sheet resistance kept increasing (curve c). So it may be thought that the increase of sheet resistance after tape test is partially due to the residue of adhesive materials from tape.

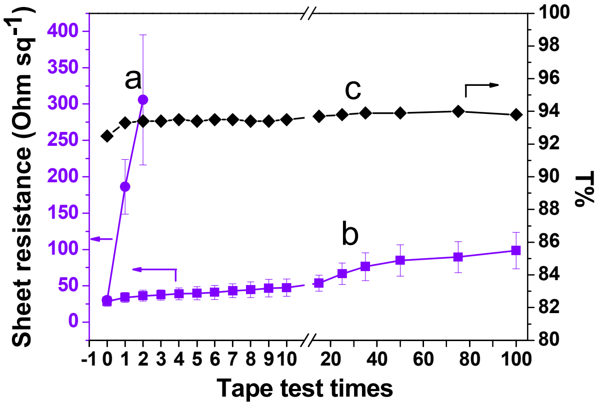

Fig. 4. Variation of sheet resistance of (a) pristine AgNW, (b) AgNW/Aa-PDA film, and (c) the corresponding transmittance at 550 nm of AgNW/Aa-PDA (b) as a function of peeling times.

In Fig. 5a, AgNW composite films with different density exhibited different optical transmittance, and it maintains constant over the entire visible spectra. In general, the optical transmittance and sheet resistance are expressed by

$$T(\lambda) = \left(1 + \frac{188.5}{R_s} \frac{\sigma_{\mathrm{Op}}(\lambda)}{\sigma_{\mathrm{DC}}}\right)^{-2} \tag{1}$$

where $\sigma_{\mathrm{Op}}(\lambda)$ is the optical conductivity and σ_{DC} is the DC conductivity of the film. The transparent electrode can be rated by a Figure of merit (FoM), the ratio of DC to optical conductivity ($\sigma_{\mathrm{DC}}/\sigma_{\mathrm{Op}}$). For high-performance electrode, it is desired to maintain a low surface resistivity and a high optical transmission, which corresponds to a higher value of $\sigma_{\mathrm{DC}}/\sigma_{\mathrm{Op}}$. Previous study revealed a value of $\sigma_{\mathrm{DC}}/\sigma_{\mathrm{Op}}$ ~350 for AgNW networks, which is much higher than those of other transparent conducting materials, such as PEDOT:PSS ($\sigma_{\mathrm{DC}}/\sigma_{\mathrm{Op}} \approx 25$),[28] single-walled CNTs (SWNTs) ($\sigma_{\mathrm{DC}}/\sigma_{\mathrm{Op}} \approx 25$)[5] and graphene ($\sigma_{\mathrm{DC}}/\sigma_{\mathrm{Op}} \approx 70$).[29] But when took adhesion into consideration, this value sharply reduced to 50~85 at high transmittance.[11, 22, 21] The reported best $\sigma_{\mathrm{DC}}/\sigma_{\mathrm{Op}}$ value is near 150 for $T \sim 87\%$, which obtained from AgNW film encapsulated with conducting PEDOT:PSS by two-step spray-coating.[30] Our AgNW composite films display a $\sigma_{\mathrm{DC}}/\sigma_{\mathrm{Op}}$ value of 200 in the range of $T = 79\%\sim89\%$, and still up to 160 at $T \sim 92\%$ (Fig. 5b). These values were much higher than that of commercial ITO on PET ($\sigma_{\mathrm{DC}}/\sigma_{\mathrm{Op}} = 100$) and the spray-coated pristine AgNW networks whose σ_{DC}/σ_{Op} = 50-75 at high transmittance.[17]

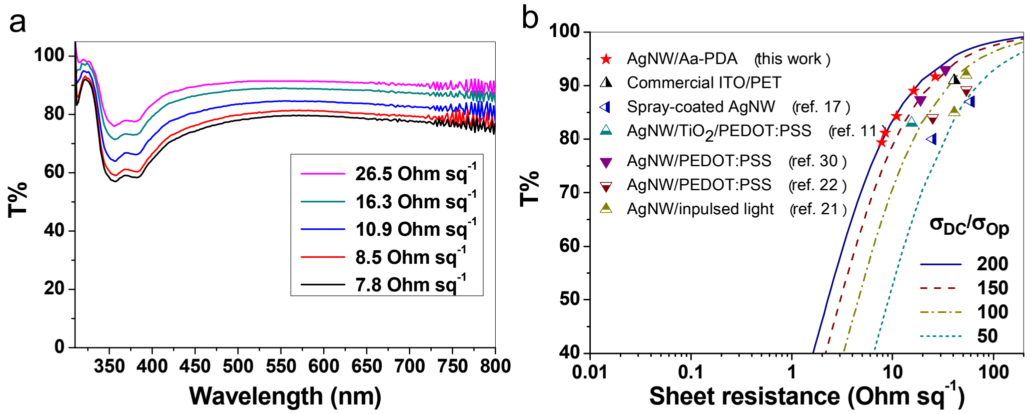

Fig. 5. (a) Optical transmission spectra of AgNW/Aa-PDA film. (b) Plot of optical transmittance versus sheet resistance. The previous reported values were also shown for comparison.

The SEM images of AgNWs before and after adding Aa-PDA was revealed to further study the reason of performance improvement (seen in Fig. 6). It shows the clear difference between AgNW and AgNW/Aa-PDA composite film. In the pristine AgNW film (Fig. 6a), Ag nanowire loosely stacked on the neighboring ones or substrate with limited point or line contact. Therefore, it is possible to cause the poor electrical conductivity if high-temperature thermal annealing or other post-treatment was not applied. Furthermore, many nanowires were suspended on the substrate without direct contact, potentially leading to weak adhesion of pristine AgNW to substrate or to other nanowires. The SEM images in Fig. 6b reveals the noticeable conformal shape deformation of upper Ag nanowires along the top surface of lower nanowires due to the strong adhesive force induced by drying of Aa-PDA on AgNW percolation networks during spray coating. Hence, the contact area between crossing

Ag nanowires was dramatically enlarged, and thus yielding strengthened electrical contact between Ag nanowires. Moreover, the AgNWs also contacted with substrate conformally after Aa-PDA was added, which possibly yielded strengthened adhesion to substrate. It is noted that obvious shine is always observed at the crossed position of pristine AgNW film, and clearly decreased or disappeared for AgNW/Aa-PDA composite film. Generally, sample with poor conductivity is inclined to exhibit shine edge during SEM test. In brief, the adhesion and electrical performance of AgNW networks improved by insulating Aa-PDA is noticeable revealed by above tests. We attributed this to better connections between Ag nanowires induced by Aa-PDA and effective film deposition technology of spray coating.[32]

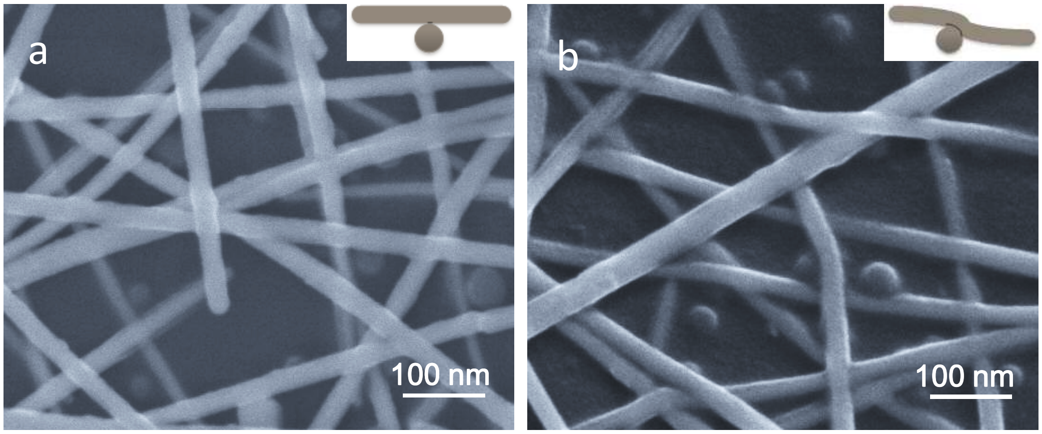

Fig. 6. SEM images of (a) pristine AgNW film, (b) AgNW/Aa-PDA composite film on PET. Insets are the corresponding schematics of Ag nanowire shape deformation.

Although many groups have been involved in performance enhancement of AgNW mesh, almost none working related to the long-term reliability during high temperature and high humidity. However, the long-term reliability is one of the most important performances of AgNW film for commercial application in microelectronics, and it encounters much greater challenge when adhesive polymer is added into AgNW film. Because good solubility or dispersibility in low-volatile solvent is usually required for adhesive polymer so as to fulfill solution-processed deposition technology of AgNW film, consequently lower the resistance against humidity. Dong et al. first investigated the long-term stability of AgNW/PEDOT:PSS hybrid film in air at 25.5 ± 0.95 °C and 49.5 ± 4.5% RH, and the resistance was increased by 9.3 – 24.7% after near 40 h.[30] In this paper, we studied the conductivity change of the pristine AgNW film and the fabricated AgNW/Aa-PDA film during 85 °C/85%RH aging for 30 days. As depicted in Fig. 7, the sheet resistance didn't show an increase trend from the beginning. On the contrary, it dropped from 24.0 to 19.9 Ohm sq^{-1} during the first 8 days for AgNW/Aa-PDA composite film, and maintained a gentle raise during the following days, which was still lower than the original value. The conductivity variation of AgNW/Aa-PDA composite film doesn't show obvious difference with that of pristine AgNW film. It indicated that the long-term stability of our film can meet the essential requirement for microelectronics application. The reduction of sheet resistance during aging may be due to the further sintering of crossing Ag nanowires caused by heating and shrinkage of Aa-PDA at 85 °C.

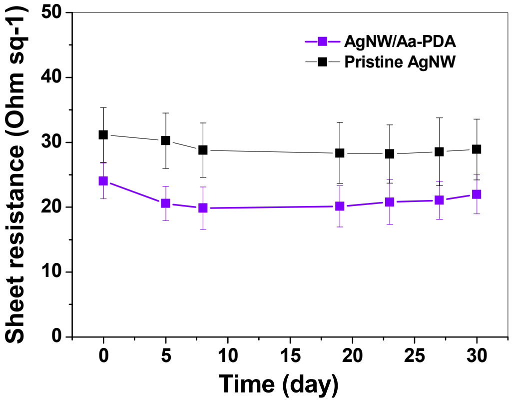

Fig. 7. Variations of sheet resistance over the 85 °C/85%RH aging.

Generally, solution processing will be conducted on the surface of AgNW film during a device fabrication. Thus, the additive in AgNW composite is expected to resist solvent to remainits adhesion in the following solution process. In Fig. 8a, we studied the solvent resistance of pristine AgNW and AgNW/Aa-PDA against acetone, water and isopropyl alcohol (IPA). The sheet resistances of pristine AgNW and AgNW/Aa-PDA films didn't show great change when exposure to acetone and water for 11 hours. By contrast, the sheet resistance exhibited a slight decrease of , which is similar with other report.[10] The stabilities of AgNW films in IPA are not as good as that in acetone and water. The sheet resistance of AgNW/Aa-PDA composite film increased by 18% after immersion in IPA for 6 hours, while it increased by 40% for pristine AgNW film after 2 hours' immersion. The relatively inferior performance of AgNW against IPA may be due to the swelling or dissolution of Aa-PDA and the stabilizer on AgNW surface in IPA. The AgNW/Aa-PDA film was also studied by tape test after immersion in acetone, water and IPA for 6 h, respectively. As depicted in Fig. 8b, the sheet resistance only changed by 15% for acetone, 27% for water, which is higher than that of the as-prepared AgNW/Aa-PDA film after tape test, but still in the range of the requirement of lower than 30%. But the sheet resistance increased by 41% after tape test for IPA immersion. In conclusion, the AgNW/Aa-PDA composite films have a good endurance against acetone and water, but weaker resistance to IPA. Thus, IPA should be carefully chosen as the solvent for the following solution process during device fabrication.

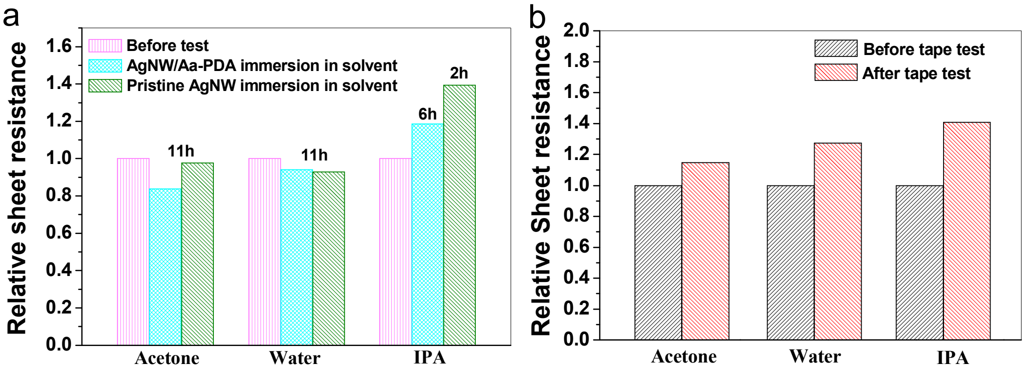

Fig. 8. (a) Variation of sheet resistance of AgNW/Aa-PDA after exposure to acetone for 11 h, water for 11 h and IPA for 6 h, respectively. (b) Sheet resistance changes after immersion in acetone, water and IPA for 6 h followed by tape test.

As application for flexible electronics, the flexibility of TCF is also very important. It is known that ITO tends to crack during bending due to its brittle nature. As revealed in Fig. 9, the sheet resistance of ITO on PET substrate dramatically increased to hundreds of Ohm per square after two bending cycles, while it only increased by 4.9% for AgNW/Aa-PDA film over 1000 bending cycles, which is similar with that of pristine AgNW film.[13,16]

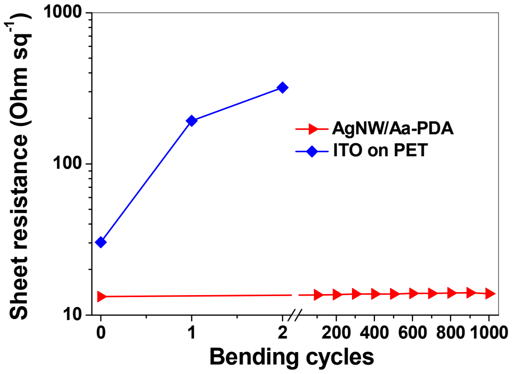

Fig. 9. Sheet resistances over the bending cycle of AgNW/Aa-PDA film and ITO on PET substrate, the bending radius is 3.1 mm.

CONCLUSIONS

We fabricated high-performance AgNW composite film using complex of alginic acid and poly(dopamine) as adhesive polymer via a simple and fast one-step spray coating technique at room temperature. The drying of Aa-PDA on the Ag nanowire percolation network noticeably enhanced the electrical conductivity and adhesion strength of AgNW mesh on the low-cost PET substrate. Highly flexible transparent electrode was obtained, not only showing better optical and electrical performance than that of commercial ITO on PET substrate, but also strong resistance against multiple tape tests. Most importantly, it exhibited good stability in organic or inorganic solvent and excellent long-term reliability during 85 °C/85%RH aging. The AgNW films demonstrated here possess attractive comprehensive performance for application as transparent electrode in emerging flexible electronic devices.

Acknowledgements

This study was supported by National Science and Technology Major Project with Contracts 2011ZX02602 and 2013ZX02505.

Notes and references

1 M. Vosgueritchian, D. J. Lipomi, Z. Bao, *Adv. Funct. Mater.* 2012**,** **22**, 421-428.

2 H. Y. Chen, H. P. Shen, C. H. Wu, W. Y. Chiu, W. C. Chen, H. J. Tai, *J. Mater. Chem. C* 2013, **1**, 5351-5358.

3 Y. Xia, J. Ouyang, *Macromolecules* 2009, **42**, 4141-4147.

4 Q. Cao, J. A. Rogers, *Adv. Mater.* 2009, **21**, 29-53.

5 H. Z. Geng, D. S. Lee, K. K. Kim, G. H. Han, H. K. Park, Y. H. Lee, *Chem. Phys. Lett.* 2008, **455**, 275-278.

6 S. Pang, Y. Hernandez, X. Feng, K. Müllen, *Adv. Mater.* 2011, **23**, 2779-2795.

7 I. K. Moon, J. I. Kim, H. Lee, K. Hur, W. C. Kim, H. Lee, *Sci. Rep.* 2013, **3**, 1112

8 M. G. Kang, L. J. Guo, *Adv. Mater.* 2007, **19**, 1391-1396.

9 P. B. Catrysse, S. Fan, *Nano Lett.* 2010, **10**, 2944-2949.

10 L. Hu, H. S. Kim, J. Y. Lee, P. Peumans, Y. Cui, *ACS Nano* 2010, **4**, 2955-2963.

11 R. Zhu, C. H. Chung, K. C. Cha, W. Yang, Y. B. Zheng, H. Zhou, T. B. Song, C. C. Chen, P. S. Weiss, G. Li, Y. Yang, *ACS Nano* 2011, **5**, 9877-9882.

12 Z. Yu, Q. Zhang, L. Li, Q. Chen, X. Niu, J. Liu, Q. Pei, *Adv. Mater.* 2011, **23**, 664-668.

13 L. Hu, H. Wu, Y. Cui, *Mrs Bull.* 2011, **36**, 760-765.

14 J. Lee, I. Lee, T. S. Kim, J. Y. Lee, *Small* 2013, **9**, 2887-94.

15 A. Kumar, C. Zhou, *ACS Nano* 2010, **4**, 11-14.

16 S. De, T. M. Higgins, P. E. Lyons, E. M. Doherty, P. N. Nirmalraj, W. J. Blau, J. J. Boland, J. N. Coleman, *ACS Nano* 2009, **3**, 1767-1774.

17 A. R. Madaria, A. Kumar, C. Zhou, *Nanotechnology* 2011, **22**, 245201-245208.

18 A. Madaria, A. Kumar, F. Ishikawa, C. Zhou, *Nano Res.* 2010, **3**, 564-573.

19 J. Y. Lee, S. T. Connor, Y. Cui, P. Peumans, *Nano Lett.* 2008, **8**, 689-692.

20 M. Hu, J. Gao, Y. Dong, K. Li, G. Shan, S. Yang, R. K. Li, *Langmuir* 2012, **28**,

7101-7106.

21 J. Jiu, M. Nogi, T. Sugahara, T. Tokuno, T. Araki, N. Komoda, K. Suganuma, H. Uchida, K. Shinozaki, *J. Mater. Chem.* 2012, **22**, 23561-23567.

22 J. Lee, P. Lee, H. B. Lee, S. Hong, I. Lee, J. Yeo, S. S. Lee, T. S. Kim, D. Lee, S. H. Ko, *Adv. Funct. Mater.* 2013, **23**, 4171-4176.

23 H. Lee, S. M. Dellatore, W. M. Miller, P. B. Messersmith, *Science* 2007, **318**, 426-430.

24 T. Akter, W. S. Kim, *ACS Appl. Mater. Inter.* 2012, **4**, 1855-1859.

25 H. Jiang, K. S. Moon, Y. Li, C. P. Wong, *Chem. Mater.* 2006, **18**, 2969-2973.

26 K. Ankireddy, S. Vunnam, J. Kellar, W. Cross, *J. Mater. Chem. C* 2013, **1**, 572-579.

27 I. Kovalenko, B. Zdyrko, A. Magasinski, B. Hertzberg, Z. Milicev, R. Burtovyy, I. Luzinov, G. Yushin, *Science* 2011, **334**, 75-79.

28 Y. H. Kim, C. Sachse, M. L. Machala, C. May, L. M. Meskamp, K. Leo, *Adv. Funct. Mater.* 2011, **21**, 1076-1081.

29 S. Bae, H. Kim, Y. Lee, X. Xu, J. S. Park, Y. Zheng, J. Balakrishnan, T. Lei, H. R. Kim, Y. I. Song, *Nat. Nanotechnol.* 2010, **5**, 574-578.

30 D. Y. Choi, H. W. Kang, H. J. Sung, S. S. Kim, *Nanoscale* 2013, **5**, 977-983.

31 W. Gaynor, J. Y. Lee, P. Peumans, *ACS nano* 2009, **4**, 30-34.

32 V. Scardaci, R. Coull, P. E. Lyons, D. Rickard and J. N. Coleman, *Small* 2011,**7**, 2621-2628.

Graphical Table of Contents